

FREE VIBRATION OF LAMINATED COMPOSITE RECTANGULAR PLATES

MOHAMAD S. QATU

Test and Analysis Group, DRESSER Industries, 274 East First Avenue, Columbus,
OH 43201, U.S.A.

(Received 22 August 1990; in revised form 24 January 1991)

Abstract—The Ritz method with algebraic polynomial displacement functions is used to solve the vibration problem for laminated composite plates having different boundary conditions. Natural frequencies and mode shapes for plates having two adjacent free edges and the remaining edges either simply supported, clamped or free are presented. Convergence studies are made which demonstrate that accurate results are obtained by using 64 displacement terms for symmetrically-laminated plates. The effects of various parameters (material, fiber orientation and boundary conditions) upon the natural frequencies and mode shapes are studied.

I. INTRODUCTION

Laminated composite structures are becoming increasingly important in many engineering applications. The need for more information on the behavior of laminated structural components, like plates, is clear. Rectangular plates are used in many engineering applications.

The literature on the title problem is vast. A series of publications (Leissa, 1978, 1981, 1987) listed hundreds of publications on the subject. Many of the previous studies concentrate on the theory of the subject, obtaining natural frequencies only for those problems which permit exact solutions (Jones, 1973; Lin, 1974). Exact Navier-type solutions are possible for cross-ply plates having shear diaphragm boundaries (Jones, 1973) and antisymmetric angle-ply plates having a certain type of simple-support boundaries (S3). Exact Levy-type solutions are also possible for cross-ply laminates having two opposite shear diaphragm edges and for antisymmetric angle-ply laminates having two opposite S3 boundaries (Lin and King, 1979). Limited references are available on the study of the effects of many parameters like the material orthotropic characteristics, the number of layers, the lamination angle and boundary conditions on the natural frequencies and mode shapes of composite plates (Leissa and Narita, 1989).

Simply-supported, symmetrically-laminated plates were recently studied (Leissa and Narita, 1989). The first eight natural frequencies and mode shapes were obtained. The Ritz method with trigonometric functions was used and reasonably accurate and comprehensive results were obtained. Symmetrically-laminated cantilevered plates were also analyzed in another study (Jensen *et al.*, 1982; Jensen and Crawley, 1984). Experimental and analytical natural frequencies and mode shapes were obtained. The finite element and the Ritz methods with beam and plate functions were used. Completely-free, symmetrically-laminated plates were recently analyzed (Sivakumaran, 1987). Frequencies obtained by using the finite element method and those obtained by using the Ritz method with algebraic polynomials were compared with experimental results.

A complete and mathematically-consistent set of equations, including equations of motion, boundary conditions and energy functionals, was presented recently for shallow shells and can be easily specialized for plates (Qatu, 1989; Leissa and Qatu, 1991). It is shown there that the energy functionals derived are consistent with the equations of motion and boundary conditions, and therefore can be used with energy approaches such as the Ritz method. These equations were successfully applied to obtain the natural frequencies of laminated cantilevered and completely free plates and shallow shells (Qatu, 1989; Qatu and Leissa, 1991a, b). The Ritz method with algebraic polynomials was used.

The main objective of this study is to present a procedure for solving the vibration problem of composite plates with various boundary conditions. This procedure is based on the Ritz method and uses algebraic polynomials. Among the other objectives of this paper is to present the first known, reasonably-accurate, natural frequencies and mode shapes of laminated plates with certain boundary conditions and to study the effects of many parameters like the lamination angle and orthotropy ratio on the natural frequencies and mode shapes of these plates.

2. ANALYSIS

The Ritz method may be used to solve the free vibration problem. This utilizes the strain energy and kinetic energy functionals for laminated plates. The strain energy stored in the plate during elastic deformation may be written in terms of the middle surface displacements u and v in directions tangential to the middle surface and parallel to the xz - and yz -planes, respectively, and the normal displacement w (see Fig. 1). The strain energy is (Qatu, 1989; Leissa and Qatu, 1991):

$$\begin{aligned}
 U = \frac{1}{2} \iint \left\{ & A_{11} \left(\frac{\partial u}{\partial x} \right)^2 + A_{22} \left(\frac{\partial v}{\partial y} \right)^2 + A_{66} \left\{ \left(\frac{\partial u}{\partial y} \right)^2 + 2 \left(\frac{\partial u}{\partial x} \frac{\partial v}{\partial y} \right) + \left(\frac{\partial v}{\partial x} \right)^2 \right\} \right. \\
 & + 2A_{12} \left(\frac{\partial u}{\partial x} \frac{\partial v}{\partial y} \right) + 2A_{16} \left(\frac{\partial u}{\partial x} \frac{\partial u}{\partial y} + \frac{\partial u}{\partial x} \frac{\partial v}{\partial x} \right) + 2A_{26} \left(\frac{\partial u}{\partial y} \frac{\partial v}{\partial y} + \frac{\partial v}{\partial x} \frac{\partial v}{\partial y} \right) \\
 & + D_{11} \left(\frac{\partial^2 w}{\partial x^2} \right)^2 + D_{22} \left(\frac{\partial^2 w}{\partial y^2} \right)^2 + 2D_{12} \left(\frac{\partial^2 w}{\partial x^2} \right) \left(\frac{\partial^2 w}{\partial y^2} \right) + 4D_{66} \left(\frac{\partial^2 w}{\partial x \partial y} \right)^2 \\
 & + 4D_{16} \left(\frac{\partial^2 w}{\partial x^2} \right) \left(\frac{\partial^2 w}{\partial x \partial y} \right) + 4D_{26} \left(\frac{\partial^2 w}{\partial y^2} \right) \left(\frac{\partial^2 w}{\partial x \partial y} \right) \\
 & - 2 \left(B_{16} \frac{\partial v}{\partial x} \frac{\partial^2 w}{\partial x^2} + 2B_{26} \frac{\partial v}{\partial y} \frac{\partial^2 w}{\partial x \partial y} + B_{26} \frac{\partial v}{\partial x} \frac{\partial^2 w}{\partial y^2} \right) \\
 & - 2 \left(B_{12} \frac{\partial v}{\partial y} \frac{\partial^2 w}{\partial x^2} + 2B_{66} \frac{\partial v}{\partial x} \frac{\partial^2 w}{\partial x \partial y} + B_{22} \frac{\partial v}{\partial y} \frac{\partial^2 w}{\partial y^2} \right) \\
 & - 2 \left(B_{11} \frac{\partial u}{\partial x} \frac{\partial^2 w}{\partial x^2} + 2B_{66} \frac{\partial u}{\partial y} \frac{\partial^2 w}{\partial x \partial y} + B_{12} \frac{\partial u}{\partial x} \frac{\partial^2 w}{\partial y^2} \right) \\
 & \left. - 2 \left(B_{16} \frac{\partial u}{\partial y} \frac{\partial^2 w}{\partial x^2} + 2B_{16} \frac{\partial u}{\partial x} \frac{\partial^2 w}{\partial x \partial y} + B_{26} \frac{\partial u}{\partial y} \frac{\partial^2 w}{\partial y^2} \right) \right\} dx dy \tag{1}
 \end{aligned}$$

where the A_{ij} , B_{ij} and D_{ij} are the conventional laminate stiffness coefficients (Vinson and Sierakowski, 1986).

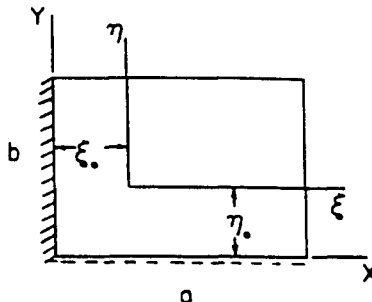


Fig. 1. Non-dimensional coordinates for a CSFF plate.

The above energy functional may be expressed in terms of middle surface strains and curvature changes which are related to the middle surface displacements by

$$\begin{aligned} \varepsilon_x &= \frac{\partial u}{\partial x}, \quad \varepsilon_y = \frac{\partial v}{\partial y}, \quad \gamma_{xy} = \frac{\partial v}{\partial x} + \frac{\partial u}{\partial y} \\ \kappa_x &= -\frac{\partial^2 w}{\partial x^2}, \quad \kappa_y = -\frac{\partial^2 w}{\partial y^2}, \quad \tau = -2\frac{\partial^2 w}{\partial x \partial y}. \end{aligned} \quad (2)$$

The total kinetic energy is

$$T = \frac{\rho}{2} \iint \{\dot{u}_0^2 + \dot{v}_0^2 + \dot{w}_0^2\} dx dy \quad (3)$$

where ρ is the average mass density of the composite plate per unit volume.

For free vibrations of a shallow shell having the rectangular planform shown in Fig. 1, displacements are assumed as:

$$\begin{aligned} u(x, y, t) &= U(x, y) \sin \omega t \\ v(x, y, t) &= V(x, y) \sin \omega t \\ w(x, y, t) &= W(x, y) \sin \omega t. \end{aligned} \quad (4)$$

Algebraic trial functions will be used in the analysis because first, they do form a complete set of functions, which guarantees convergence to the exact solution as the number of terms taken increases and, second, one can straightforwardly solve for many boundary conditions using algebraic trial functions.

The displacement functions U , V and W can be written in terms of the non-dimensional coordinates ξ and η as:

$$\begin{aligned} U(\xi, \eta) &= \sum_{i=i_0}^I \sum_{j=j_0}^J \alpha_{ij} \xi^i \eta^j \\ V(\xi, \eta) &= \sum_{k=k_0}^K \sum_{l=l_0}^L \beta_{kl} \xi^k \eta^l \\ W(\xi, \eta) &= \sum_{m=m_0}^M \sum_{n=n_0}^N \gamma_{mn} \xi^m \eta^n \end{aligned} \quad (5)$$

where $\xi = x/a - \xi_0$ and $\eta = y/b - \eta_0$ and ξ_0, η_0 are defined in Fig. 1.

Keeping in mind that the Ritz method requires satisfaction of geometric (forced) boundary conditions only, with suitable selection of the values $\xi_0, \eta_0, i_0, j_0, k_0, l_0, m_0$ and n_0 one can solve for many boundary conditions with the same analytical procedure. Vibration problems for laminated plates having the boundary conditions $XXXX$, where X can be simply supported (S), clamped (C), or free (F), can be solved. One should keep in mind that for generally-laminated plates there are four types of boundary conditions for each of the S, F and C edge conditions (as described in Table 1).

Table 1 shows the combinations of i_0, k_0 and m_0 that should be used in the x -direction to get each of the possible boundary conditions at $x = 0$. Similar types of boundary conditions can be obtained at $y = 0$ by suitable selection of j_0, l_0 and n_0 . This will enable one to solve for six boundary conditions of isotropic, orthotropic or anisotropic laminated plates, namely, FFFF, SFFF, SSFF, CFFF, CSFF and CCFF. It will also enable one to solve for 78 combinations of boundary conditions of unsymmetrically-laminated plates.

For solving the free vibration problem, eqns (4) and (5) are substituted into eqn (1) in order to get an expression for the maximum strain energy (U_{\max}) and into (3) in order to get an expression for the maximum kinetic energy (T_{\max}).

Table 1. Values of i_0 , k_0 and m_0 needed to get different boundary conditions at $x = 0$ (similar types of boundary conditions can be obtained at $y = 0$ by suitable selection of j_0 , l_0 and n_0)

| B.C. at $x = 0$ | i_0 | k_0 | m_0 |
|-----------------|-------|-------|-------|
| F-1 | 1 | 1 | 0 |
| F-2 | 0 | 1 | 0 |
| F-3 | 1 | 0 | 0 |
| F-4 | 0 | 0 | 0 |
| S-1 | 1 | 1 | 1 |
| S-2 | 0 | 1 | 1 |
| S-3 | 1 | 0 | 1 |
| S-4 | 0 | 0 | 1 |
| C-1 | 1 | 1 | 2 |
| C-2 | 0 | 1 | 2 |
| C-3 | 1 | 0 | 2 |
| C-4 | 0 | 0 | 2 |

The Ritz method requires minimization of the functional $(T_{\max} - U_{\max})$ with respect to the coefficient α_{ij} , β_{kl} and γ_{mn} which can be accomplished by setting:

$$\begin{aligned} \frac{\partial(T_{\max} - U_{\max})}{\partial\alpha_{ij}} &= 0 \quad i = i_0, i_0 + 1, \dots, I; \quad j = j_0, j_0 + 1, \dots, J \\ \frac{\partial(T_{\max} - U_{\max})}{\partial\beta_{kl}} &= 0 \quad k = k_0, k_0 + 1, \dots, K; \quad l = l_0, l_0 + 1, \dots, L \\ \frac{\partial(T_{\max} - U_{\max})}{\partial\gamma_{mn}} &= 0 \quad m = m_0, m_0 + 1, \dots, M; \quad n = n_0, n_0 + 1, \dots, N \end{aligned} \quad (6)$$

which yields a total of $(I - i_0 + 1) \times (J - j_0 + 1) + (K - k_0 + 1) \times (L - l_0 + 1) + (M - m_0 + 1) \times (N - n_0 + 1)$ simultaneous, linear, homogeneous equations in an equal number of unknowns α_{ij} , β_{kl} and γ_{mn} . Those equations can be described by:

$$(K - \Omega^2 M) \mathbf{a} = 0 \quad (7)$$

where K and M are the stiffness and mass matrices, respectively; Ω is the frequency parameter, and \mathbf{a} is the vector of unknown coefficients α_{ij} , β_{kl} and γ_{mn} .

The determinant of the coefficient matrix is set equal to zero which will yield a set of eigenvalues. Substituting each eigenvalue back into eqns (5) yields the corresponding eigenvector (amplitude ratio) in the usual manner. The mode shape corresponding to each frequency can be determined by substituting the eigenvector back into eqns (5).

It has been noted that the convergence characteristics and possible matrix ill-conditioning can be improved if one uses the non-dimensional coordinates such that they form planes of symmetry. This can be done for the completely free, SSFF and cantilever plates. For that reason, $\xi_0 = \eta_0 = 1/2$ are used for completely free boundaries, where two lines of symmetry are observed, $\xi_0 = 0$ and $\eta_0 = 1/2$ are used for SSFF and CFFF boundaries, where one line of symmetry is observed, and $\xi_0 = \eta_0 = 0$ are used for SSFF, CSFF and CCFF boundary conditions. For the SSFF and CCFF plates, there exists a diagonal line of symmetry which cannot be accounted for easily with the present polynomials. It should also be mentioned that the symmetry is preserved only for isotropic or orthotropic rectangular plates, and is lost for generally anisotropic plates.

For symmetrically laminated plates all of the stretching-bending coupling (i.e. $B_{ij} = 0$) terms vanish. This leads to decoupling the in-plane displacements from the out-of-plane displacements. The possible combination of boundary conditions which can be solved by

Table 2. Values of m_0 and n_0 for various boundary conditions at $x = 0$ and $y = 0$

| B.C. | m_0 | n_0 |
|------|-------|-------|
| FFFF | 0 | 0 |
| SFFF | 1 | 0 |
| CFFF | 2 | 0 |
| SSFF | 1 | 1 |
| CSFF | 2 | 1 |
| CCFF | 2 | 2 |

the present method reduces to six as was mentioned earlier. Only the last equations of the sets of eqns (4), (5) and (6) are needed for the transverse vibrations. This leads to a system of linear, homogeneous equations of the order $(M - m_0 + 1) \times (N - n_0 + 1)$. Table 2 gives the required values of m_0 and n_0 for each of the six combinations of boundary conditions.

Comparisons among results from the present method and analytical and experimental data obtained by Jensen *et al.* (1982) for laminated cantilever plates may be found in the dissertation by Qatu (1989) and the work accomplished by Qatu and Leissa (1991a). There, the natural frequencies obtained experimentally, and those obtained by using the finite element method, are compared with those obtained by the present method. Different lamination and aspect ratios for plates having eight plies are included in those studies. It was concluded that the present method yields a closer upper bound to the exact solution than the finite element results, and is reasonably close to the frequencies obtained experimentally. The Ritz method with algebraic polynomials yielded closer upper bounds to the exact solutions than the Ritz method with certain beam and plate functions. Other comparisons were made with the experimental and analytical results for completely-free plates given by Sivakumaran (1987). These comparisons can be found in the work by Qatu (1989) and Qatu and Leissa (1991b).

3. CONVERGENCE STUDIES

Convergence studies are made for composite plates representative of those to be analyzed subsequently. These include symmetric laminates of three-layers, with stacking sequence $[\theta/-\theta/\theta]$. The angle θ lies between the fibers and the projection of the x -axis upon the plate. Filamentary composite materials of two types were considered, namely E-glass/epoxy (E/E) and graphite/epoxy (G/E). The following material properties were used:

$$\text{E-glass/epoxy: } E_1 = 60.7 \text{ GPa, } E_2 = 24.8 \text{ GPa, } G_{12} = 12.0 \text{ GPa, } \nu_{12} = 0.23 \quad (8)$$

$$\text{Graphite/epoxy: } E_1 = 138 \text{ GPa, } E_2 = 8.96 \text{ GPa, } G_{12} = 7.1 \text{ GPa, } \nu_{12} = 0.30. \quad (9)$$

The above properties were taken from Vinson and Sierakowski (1986).

A typical plate of square planform ($a/b = 1$) is used. Convergence studies of the lowest eight frequency parameters $\Omega = \omega a^2 \sqrt{\rho/E_1 h^2}$ for E-glass/epoxy plates having the six boundary conditions which will subsequently be analyzed can be found in Table 3, and those for graphite/epoxy can be found in Table 4.

For both materials considered here and for each of the six boundary conditions, three solutions are presented. These solutions are obtained by using 36, 49 and 64 terms for the first, second and third solutions, respectively. Equal numbers of terms are taken in each of the in-plane directions.

Convergence is observed to be reasonably good for engineering applications. The maximum difference between the 49- and the 64-term solutions is less than 3% for all the cases. The set of boundary conditions with the poorest convergence is the completely free one. As geometric constraints are imposed on the boundaries, convergence seems to improve and the fastest convergence is observed for the plate with two adjacent clamped edges (i.e.

Table 3. Convergence of the frequency parameter Ω for E-glass epoxy square plates

| B.C. | Deter. size | Ω | | | | | | | | |
|------|-------------|----------|--------|--------|--------|--------|--------|--------|--------|--|
| FFFF | 36 | 3.1565 | 4.2313 | 5.9894 | 7.4964 | 9.0989 | 12.754 | 14.610 | 16.146 | |
| | 49 | 3.1548 | 4.1999 | 5.9283 | 7.3904 | 8.9624 | 12.735 | 14.157 | 16.119 | |
| | 64 | 3.1547 | 4.1999 | 5.9282 | 7.3898 | 8.9459 | 12.368 | 14.038 | 15.654 | |
| SFFF | 36 | 1.5929 | 3.8429 | 5.3387 | 6.4864 | 11.245 | 12.795 | 13.513 | 15.820 | |
| | 49 | 1.5928 | 3.8418 | 5.2989 | 6.4644 | 11.069 | 12.643 | 13.484 | 15.620 | |
| | 64 | 1.5928 | 3.8417 | 5.2989 | 6.4633 | 11.051 | 12.640 | 13.153 | 15.527 | |
| CFFF | 36 | 0.8672 | 2.1074 | 5.3240 | 5.9287 | 7.7640 | 12.572 | 14.029 | 15.508 | |
| | 49 | 0.8668 | 2.1071 | 5.3094 | 5.8832 | 7.7558 | 12.388 | 14.012 | 15.492 | |
| | 64 | 0.8667 | 2.1065 | 5.3090 | 5.8827 | 7.7529 | 12.309 | 14.691 | 15.486 | |
| SSFF | 36 | 0.7815 | 3.6549 | 4.9662 | 8.6598 | 11.047 | 13.644 | 15.694 | 19.037 | |
| | 49 | 0.7814 | 3.6549 | 4.9657 | 8.6509 | 10.940 | 13.507 | 15.561 | 18.808 | |
| | 64 | 0.7802 | 3.6547 | 4.9650 | 8.6506 | 10.938 | 13.503 | 15.553 | 18.763 | |
| CSFF | 36 | 1.3857 | 4.1729 | 6.4700 | 9.8837 | 11.536 | 16.318 | 17.209 | 21.114 | |
| | 49 | 1.3856 | 4.1724 | 6.4690 | 9.8563 | 11.450 | 16.285 | 17.111 | 21.002 | |
| | 64 | 1.3855 | 4.1721 | 6.4688 | 9.8553 | 11.448 | 16.279 | 17.092 | 20.875 | |
| CCFF | 36 | 1.7348 | 5.2632 | 6.7900 | 11.029 | 13.428 | 16.634 | 18.612 | 22.145 | |
| | 49 | 1.7345 | 5.2618 | 6.7894 | 11.025 | 13.427 | 16.629 | 18.591 | 22.070 | |
| | 64 | 1.7345 | 5.2606 | 6.7893 | 11.024 | 13.422 | 16.622 | 18.584 | 22.055 | |

CCFF plates). The maximum difference in the natural frequencies between the 49- and 64-term solutions for CCFF boundary conditions is 0.07% for E/E material and 0.14% for G/E materials.

Interestingly enough, plates with FFFF and SFFF boundaries converge faster with G/E material than do those with E/E material. While the difference between the 49- and 64-term solutions is 2.97% for E/E plates with completely free boundaries, it is 2.52% for G/E material with the same boundaries. This phenomenon is reversed for SSFF, CSFF and CCFF boundary conditions, where plates with the E/E material converge faster than those with G/E.

From the above studies, it may be considered that the 64-term solution for the plates presents satisfactory convergence for engineering applications. Therefore, 64 terms will be used in the subsequent analysis.

Table 4. Convergence of the frequency parameter Ω for graphite/epoxy square plates

| B.C. | Deter. size | Ω | | | | | | | | |
|------|-------------|----------|--------|--------|--------|--------|--------|--------|--------|--|
| FFFF | 36 | 1.6262 | 2.0910 | 3.7748 | 5.1285 | 5.1924 | 7.4462 | 7.9743 | 9.5453 | |
| | 49 | 1.6203 | 2.0789 | 3.7177 | 5.0570 | 5.1460 | 7.2263 | 7.8735 | 9.1564 | |
| | 64 | 1.6202 | 2.0784 | 3.7115 | 5.0517 | 5.0707 | 7.0800 | 7.6870 | 8.9317 | |
| SFFF | 36 | 0.9171 | 2.5554 | 3.2899 | 4.5599 | 5.8347 | 7.7369 | 9.4071 | 11.792 | |
| | 49 | 0.9166 | 2.5371 | 3.2786 | 4.5284 | 5.7501 | 7.6644 | 9.2225 | 11.255 | |
| | 64 | 0.9165 | 2.5363 | 3.2754 | 4.5181 | 5.6929 | 7.5070 | 9.0844 | 11.085 | |
| CFFF | 36 | 0.6519 | 1.4392 | 3.1581 | 4.1996 | 5.6674 | 6.7157 | 8.8263 | 11.058 | |
| | 49 | 0.6513 | 1.4377 | 3.1253 | 4.1881 | 5.6427 | 6.6344 | 8.7529 | 10.809 | |
| | 64 | 0.6507 | 1.4372 | 3.1228 | 4.1839 | 5.6111 | 6.5257 | 8.6460 | 10.557 | |
| SSFF | 36 | 0.4671 | 1.8437 | 3.9371 | 4.6707 | 6.8341 | 8.2414 | 10.919 | 12.747 | |
| | 49 | 0.4656 | 1.8248 | 3.9276 | 4.6559 | 6.7644 | 8.1051 | 10.690 | 12.395 | |
| | 64 | 0.4644 | 1.8424 | 3.9263 | 4.6541 | 6.7514 | 8.0780 | 10.540 | 12.236 | |
| CSFF | 36 | 1.0615 | 2.4227 | 5.0125 | 5.6484 | 7.9491 | 9.3699 | 12.325 | 14.282 | |
| | 49 | 1.0606 | 2.4211 | 4.9812 | 5.6388 | 7.9011 | 9.1566 | 12.059 | 13.991 | |
| | 64 | 1.0600 | 2.4205 | 4.9791 | 5.6343 | 7.8767 | 9.0771 | 11.881 | 13.713 | |
| CCFF | 36 | 1.2913 | 3.0535 | 5.5559 | 6.2780 | 8.5898 | 10.367 | 13.459 | 14.936 | |
| | 49 | 1.2912 | 3.0518 | 5.5534 | 6.2730 | 8.5715 | 10.241 | 12.990 | 14.570 | |
| | 64 | 1.2907 | 3.0495 | 5.5463 | 6.2691 | 8.5507 | 10.236 | 12.970 | 14.551 | |

4. NATURAL FREQUENCIES

Tables 5 and 6 show the lowest eight natural frequencies for E-glass/epoxy and graphite/epoxy materials, respectively. The aspect ratio (a/b) is chosen to be one indicating square plates. Three-layer $[\theta, -\theta, \theta]$ laminates are used. The lamination angle is varied from 0° to 90° with an increment of 15° . For FFFF, SSFF and CCFE square plates, symmetry about the line $\xi = \eta$ exists. This results in the frequencies for plates with the fiber angles $\theta = 60^\circ, 75^\circ$ and 90° being the same as those with the fiber angles $\theta = 30^\circ, 15^\circ$ and 0° , respectively.

It is noticed that increasing the fiber angle θ from 0° to 45° increases the lowest two non-dimensional frequencies ($\Omega = \omega b^2 \sqrt{\rho/E_1 h^2}$) for plates with geometric symmetry about the $\xi = \eta$ line (i.e. FFFF, SSFF and CCFE plates). From the symmetry of the problems, increasing the fiber angle from 45° to 90° decreases these frequencies. This indicates that the maximum fundamental frequencies are obtained with the fiber angle equal to 45° for these boundary conditions. For that angle, the fibers are parallel to the line of geometric symmetry. This observation is true for both materials considered. The effect of the orthotropy ratio is clearer for the second lowest frequency than it is for the first one. Increasing the fiber angle from 0° to 45° increases the second lowest frequency by 3.4% for E/E material and by 37% for G/E material when the boundary conditions are completely free. Similar observations are true for the other two boundary conditions (i.e. SSFF and CCFE). Mode interaction occurred for the remaining frequencies, but generally maximum frequencies occurred at the fiber angle of 45° .

For plates with the line of geometric symmetry $\eta = 0$ (i.e. SFFF and CFFF plates) the

Table 5. Frequency parameters Ω for E-glass/epoxy three-layer laminated square plates (for FFFF, SSFF and CCFE plates, natural frequencies when $\theta = 60^\circ, 75^\circ, 90^\circ$ are the same as those when $\theta = 30^\circ, 15^\circ, 0^\circ$; respectively)

| B.C. | θ (degrees) | Ω | | | | | | | |
|------|-----------------------|----------|--------|--------|--------|--------|--------|--------|--------|
| FFFF | 0 | 2.9262 | 4.1227 | 6.5314 | 7.2219 | 8.7320 | 11.504 | 14.213 | 14.419 |
| | 15 | 3.0017 | 4.1372 | 6.3438 | 7.2706 | 8.8321 | 11.668 | 13.997 | 15.039 |
| | 30 | 3.1547 | 4.1999 | 5.9282 | 7.3898 | 8.9459 | 12.368 | 14.038 | 15.654 |
| | 45 | 3.2313 | 4.2632 | 5.6855 | 7.4614 | 8.9581 | 13.492 | 14.104 | 14.142 |
| SFFF | 0 | 1.4555 | 4.4373 | 5.1290 | 6.2830 | 10.836 | 12.276 | 14.548 | 16.209 |
| | 15 | 1.4976 | 4.2707 | 5.1724 | 6.3346 | 10.904 | 12.525 | 13.977 | 15.967 |
| | 30 | 1.5928 | 3.8417 | 5.2989 | 6.4633 | 11.051 | 12.640 | 13.153 | 15.527 |
| | 45 | 1.6635 | 3.3478 | 5.4441 | 6.6407 | 11.004 | 11.311 | 13.574 | 15.620 |
| | 60 | 1.6254 | 3.0074 | 5.4827 | 6.8479 | 9.9399 | 11.252 | 13.174 | 16.651 |
| | 75 | 1.5013 | 2.8772 | 5.3539 | 7.0382 | 9.4089 | 11.245 | 12.346 | 17.821 |
| CFFF | 0 | 1.4352 | 2.8530 | 5.2546 | 7.1236 | 9.2927 | 11.400 | 11.755 | 18.487 |
| | 0 | 1.0236 | 2.0136 | 5.3729 | 6.4406 | 7.9911 | 12.304 | 12.475 | 17.967 |
| | 15 | 0.9744 | 2.0504 | 5.4406 | 6.1873 | 7.9139 | 12.240 | 12.886 | 17.206 |
| | 30 | 0.8667 | 2.1065 | 5.3090 | 5.8827 | 7.7529 | 12.309 | 13.691 | 15.486 |
| | 45 | 0.7616 | 2.0948 | 4.7185 | 6.0341 | 7.5938 | 12.354 | 13.622 | 14.641 |
| | 60 | 0.6918 | 1.9842 | 4.2966 | 6.2131 | 7.4326 | 12.110 | 12.439 | 14.855 |
| SSFF | 75 | 0.6606 | 1.8442 | 4.1217 | 6.2977 | 7.3019 | 11.588 | 12.245 | 14.130 |
| | 90 | 0.6535 | 1.7820 | 4.0846 | 6.2929 | 7.2698 | 11.460 | 12.229 | 13.707 |
| | 0 | 0.7315 | 3.6039 | 5.0009 | 8.5594 | 9.9717 | 14.938 | 15.190 | 18.463 |
| | 15 | 0.7401 | 3.6028 | 5.0269 | 8.5892 | 10.244 | 14.439 | 15.411 | 18.604 |
| | 30 | 0.7802 | 3.6547 | 4.9650 | 8.6506 | 10.938 | 13.503 | 15.553 | 18.763 |
| | 45 | 0.8037 | 3.6822 | 4.9280 | 8.6762 | 11.578 | 12.743 | 15.592 | 18.831 |
| CSFF | 0 | 1.3561 | 3.9471 | 6.8464 | 9.9789 | 10.283 | 16.377 | 18.356 | 20.187 |
| | 15 | 1.4004 | 4.0222 | 6.8104 | 9.8754 | 10.741 | 16.522 | 17.940 | 20.518 |
| | 30 | 1.3855 | 4.1721 | 6.4688 | 9.8553 | 11.448 | 16.279 | 17.092 | 20.875 |
| | 45 | 1.3068 | 4.3256 | 6.0220 | 9.7944 | 12.358 | 14.814 | 17.035 | 20.528 |
| | 60 | 1.2010 | 4.4680 | 5.6384 | 9.6604 | 12.940 | 13.960 | 16.990 | 20.005 |
| | 75 | 1.1195 | 4.5901 | 5.3820 | 9.4987 | 12.342 | 14.687 | 16.906 | 19.443 |
| CCFE | 90 | 1.0973 | 4.6999 | 5.1871 | 9.4193 | 12.076 | 15.066 | 16.878 | 19.082 |
| | 0 | 1.6104 | 5.0077 | 6.9752 | 10.854 | 12.259 | 18.008 | 18.440 | 22.040 |
| | 15 | 1.6874 | 5.0856 | 7.0032 | 10.945 | 12.600 | 16.133 | 18.411 | 22.141 |
| | 30 | 1.7345 | 5.2606 | 6.7893 | 11.024 | 13.422 | 16.622 | 18.584 | 22.055 |
| | 45 | 1.8894 | 5.3681 | 6.6448 | 11.056 | 14.257 | 15.567 | 18.683 | 22.007 |

Table 6. Frequency parameters Ω for graphite/epoxy three-layer laminated square plates (for FFFF, SSFF and CCFF plates, natural frequencies when $\theta = 60^\circ, 75^\circ, 90^\circ$ are the same as those when $\theta = 30^\circ, 15^\circ, 0^\circ$; respectively)

| B.C. | θ (degrees) | Ω | | | | | | | |
|------|-----------------------|----------|--------|--------|--------|--------|--------|--------|--------|
| FFFF | 0 | 1.4910 | 1.6461 | 3.4596 | 4.5393 | 6.4266 | 6.4713 | 7.1317 | 9.0088 |
| | 15 | 1.5234 | 1.7881 | 3.5251 | 4.7418 | 5.7179 | 6.8856 | 7.0915 | 9.0493 |
| | 30 | 1.6202 | 2.0784 | 3.7115 | 5.0517 | 5.0707 | 7.0800 | 7.6870 | 8.9317 |
| | 45 | 1.6894 | 2.2397 | 3.8250 | 4.6812 | 5.1973 | 7.2344 | 8.6974 | 8.7855 |
| SSFF | 0 | 0.7557 | 2.2394 | 4.4609 | 4.9322 | 5.1321 | 6.6056 | 9.3875 | 10.037 |
| | 15 | 0.8137 | 2.3310 | 4.0594 | 4.7834 | 5.3088 | 6.9328 | 9.0394 | 11.112 |
| | 30 | 0.9165 | 2.5363 | 3.2754 | 4.5181 | 5.6929 | 7.5070 | 9.0844 | 11.085 |
| | 45 | 0.9658 | 2.1919 | 2.9238 | 4.4457 | 5.9173 | 7.8414 | 8.1340 | 10.141 |
| | 60 | 0.9394 | 1.5457 | 2.9198 | 4.4215 | 5.7122 | 6.3606 | 8.1236 | 9.6680 |
| | 75 | 0.8292 | 1.2078 | 2.7242 | 3.9013 | 5.3423 | 6.4229 | 7.8634 | 8.6512 |
| CCFF | 0 | 0.7273 | 1.1346 | 2.5179 | 3.6786 | 5.2306 | 6.6385 | 7.6832 | 7.9838 |
| | 0 | 1.0175 | 1.3724 | 2.6393 | 5.3147 | 6.3757 | 6.8348 | 8.2455 | 10.217 |
| | 15 | 0.8717 | 1.4068 | 2.8246 | 5.4370 | 5.6820 | 6.5568 | 8.3479 | 10.164 |
| | 30 | 0.6507 | 1.4372 | 3.1228 | 4.1839 | 5.6111 | 6.5257 | 8.6460 | 10.557 |
| | 45 | 0.4607 | 1.3705 | 2.8443 | 3.4746 | 5.2594 | 6.8772 | 8.8024 | 9.1567 |
| | 60 | 0.3318 | 1.1769 | 2.0749 | 3.4072 | 5.1498 | 6.4767 | 6.9401 | 8.8053 |
| CSFF | 75 | 0.2722 | 0.9589 | 1.7073 | 3.1105 | 4.7761 | 5.9184 | 6.6539 | 8.4337 |
| | 90 | 0.2590 | 0.8622 | 1.6226 | 2.9232 | 4.5432 | 5.9732 | 6.6701 | 8.1971 |
| | 0 | 0.3727 | 1.6061 | 4.1112 | 4.6015 | 5.7303 | 8.0595 | 8.1514 | 11.884 |
| | 15 | 0.3989 | 1.6843 | 4.0683 | 4.6146 | 6.1091 | 7.7262 | 9.4298 | 11.746 |
| | 30 | 0.4644 | 1.8424 | 3.9263 | 4.6541 | 6.7514 | 8.0780 | 10.540 | 12.236 |
| | 45 | 0.4952 | 1.9058 | 3.8166 | 4.7579 | 7.1091 | 8.6320 | 10.068 | 12.175 |
| CSFF | 0 | 1.1148 | 2.0413 | 4.3747 | 6.4907 | 7.4584 | 8.2761 | 9.6074 | 13.130 |
| | 15 | 1.1585 | 2.2363 | 4.6158 | 6.2858 | 7.6601 | 8.4972 | 10.505 | 13.167 |
| | 30 | 1.0600 | 2.4205 | 4.9791 | 5.6343 | 7.8767 | 9.0771 | 10.943 | 13.713 |
| | 45 | 0.8805 | 2.5250 | 4.6162 | 5.5318 | 8.2007 | 9.5954 | 11.294 | 13.477 |
| | 60 | 0.6957 | 2.4199 | 4.3151 | 5.3569 | 7.6067 | 8.9992 | 11.434 | 12.989 |
| | 75 | 0.5619 | 2.1540 | 4.4806 | 5.0735 | 6.5309 | 8.5485 | 10.491 | 12.587 |
| CCFF | 90 | 0.5147 | 2.0392 | 4.6243 | 4.9370 | 5.9837 | 8.6892 | 9.3056 | 12.852 |
| | 0 | 1.1788 | 2.4126 | 5.1548 | 6.5157 | 7.6703 | 9.4441 | 10.134 | 14.028 |
| | 15 | 1.2801 | 2.6719 | 5.4359 | 6.3716 | 7.9964 | 9.5520 | 11.298 | 14.115 |
| | 30 | 1.2907 | 3.0495 | 5.5463 | 6.2691 | 8.5507 | 10.236 | 12.970 | 14.551 |
| | 45 | 1.2935 | 3.2985 | 5.1583 | 6.5741 | 9.2614 | 10.843 | 12.232 | 14.723 |

behavior is different. For cantilever plates, it is observed that increasing the fiber orientation angle from 0° to 90° decreases the fundamental frequency, which corresponds to the first bending mode. This effect is larger for the material with the higher orthotropy ratio (i.e. G/E). Increasing the fiber angle from 0° to 90° decreases the lowest natural frequency by 75% for G/E materials and only by 35% for E/E materials. For the second-lowest frequency, which corresponds to the first twisting mode, the maximum natural frequency is obtained when the fiber angle is 30° . The difference between the maximum second frequency (at the fiber angle $\theta = 30^\circ$) and the minimum one (at the fiber angle $\theta = 0^\circ$) is considerably larger for the plates with higher orthotropy ratio (i.e. G/E material). For SSFF plates, increasing the fiber orientation increases the fundamental frequency for the fiber angles from 0° to 45° and decreases afterwards. This indicates that the fundamental frequency for SSFF plates should be corresponding to the first twisting mode, which is what Fig. 2 shows. This observation is true for both materials, and is stronger for the G/E plates.

For CSFF plates, the geometric symmetry is lost and the fundamental frequency is observed to be maximum when the fiber angle is 15° for E/E materials and is 0° for G/E materials. This is closer to the 0° fiber angle than the 90° one because the clamped boundary condition imposes stronger constraints than does the simple-support boundary condition.

5. MODE SHAPES

Contour plots for different boundary conditions and the material with the higher orthotropy ratio (i.e. G/E) are given in Figs 2–6. Mode shapes for $\theta = 0^\circ, 15^\circ, 30^\circ, 45^\circ$ are

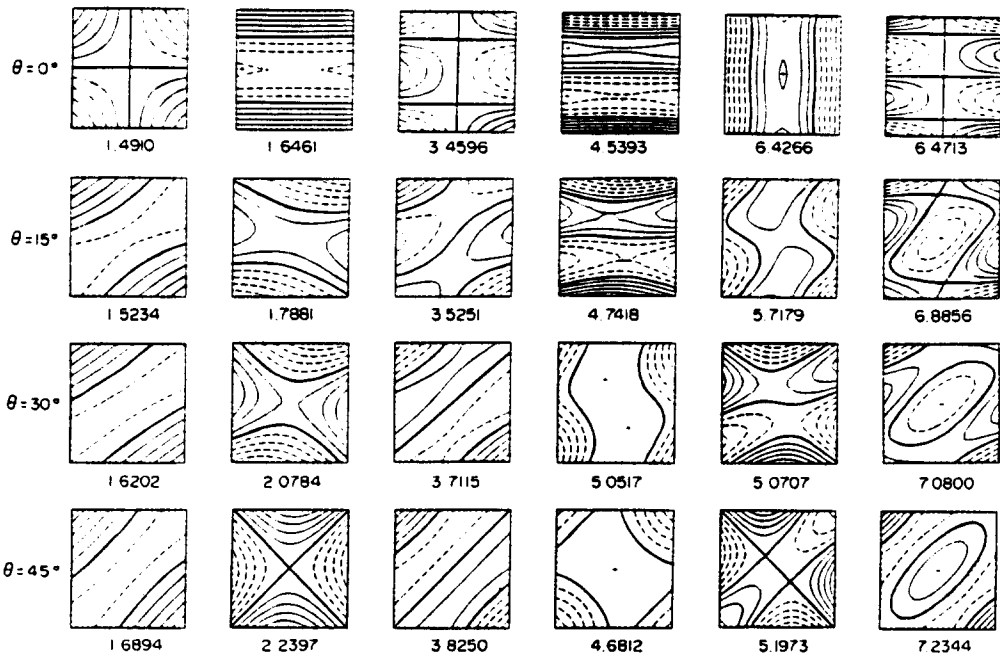


Fig. 2. Mode shapes for completely-free laminated graphite/epoxy plates.

shown for completely-free, SSFF and CCFF plates. For these boundary conditions, mode shapes for $\theta = 60^\circ$, 75° and 90° are similar to those given for $\theta = 30^\circ$, 15° and 0° , respectively, and can be easily obtained by changing the coordinates. Heavier lines in the sketches are node lines (i.e. lines of zero displacements). The absolute maximum displacement in the mode shapes is normalized to one. The displacement between the contour lines is one fifth of the maximum displacement. The first six mode shapes are given.

For the completely-free boundary condition, one should note that four possible symmetry classes exist in the displacement functions chosen. For example, one can choose $m = n = 0, 2, 4, \dots$ for the doubly-symmetric (i.e. symmetric about both the ξ and η axes) modes. Similar choices can be made for the other three symmetry classes. These symmetry classes about the ξ and η axes exist for the isotropic and cross-ply plates. This symmetry is lost for plates with angle-ply lamination and one should keep all the terms in the polynomials. For the special case of diagonally-orthotropic angle-ply laminates which are made of 45° angle layers, the symmetry classes exist about the diagonals (Fig. 2). The gradual change in contour lines with increasing θ is evident.

For plates with SFFF and CFFF boundaries, only two classes of symmetry are possible in the displacement functions (i.e. the displacement functions can be either symmetric or antisymmetric about the ζ -axis). Figures 3 and 4 give the first six mode shapes for these plates. For example, to obtain the symmetric modes one should choose $n = 0, 2, 4, \dots$. This symmetry/antisymmetry in the mode shapes can be seen for isotropic and cross-ply laminated plates. For angle-ply plates, the symmetry classes are lost and one should keep all the terms in the analysis. One should keep in mind that one zero frequency exists for SFFF plates which corresponds to the rigid-body mode. For SFFF plates with $\theta = 0$ and the fibers are parallel to the x -axis, the second mode shape is the first symmetric model with two nodal parallel to the x -axis. The equivalent to this mode when $\theta = 90^\circ$ (i.e. the fibers are perpendicular to the x -axis) is the fifth mode and the actual second mode has one nodal line in the direction of the fibers. Similar observations are made for the cantilever plates. This shows that for certain mode shapes, more nodal lines tend to appear parallel to the direction of the fibers.

Plates having CSFF boundary conditions do not permit any symmetry or antisymmetry in the mode shapes. The mode shapes tend to be similar to those obtained for plates with

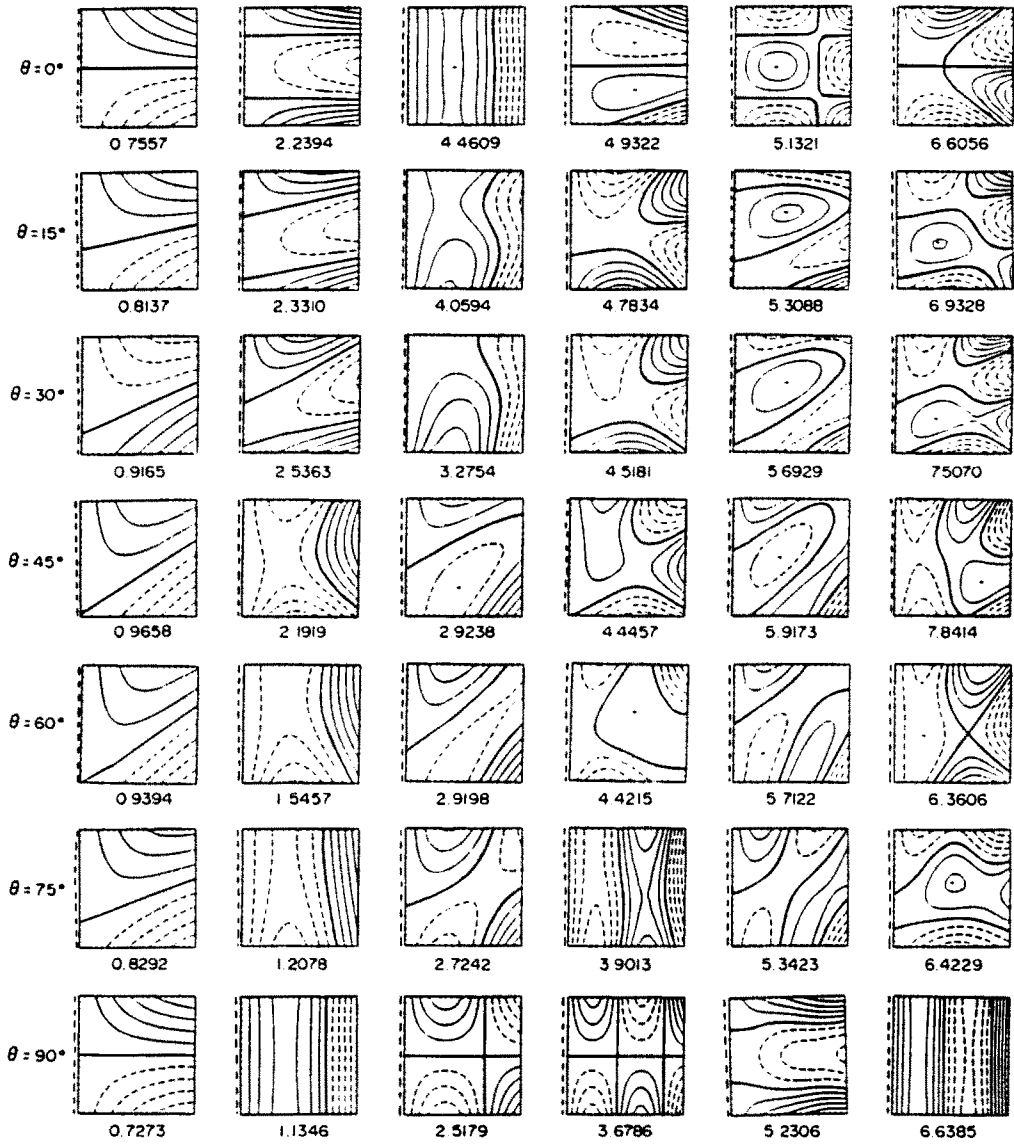


Fig. 3. Mode shapes for SFFF laminated graphite/epoxy plates.

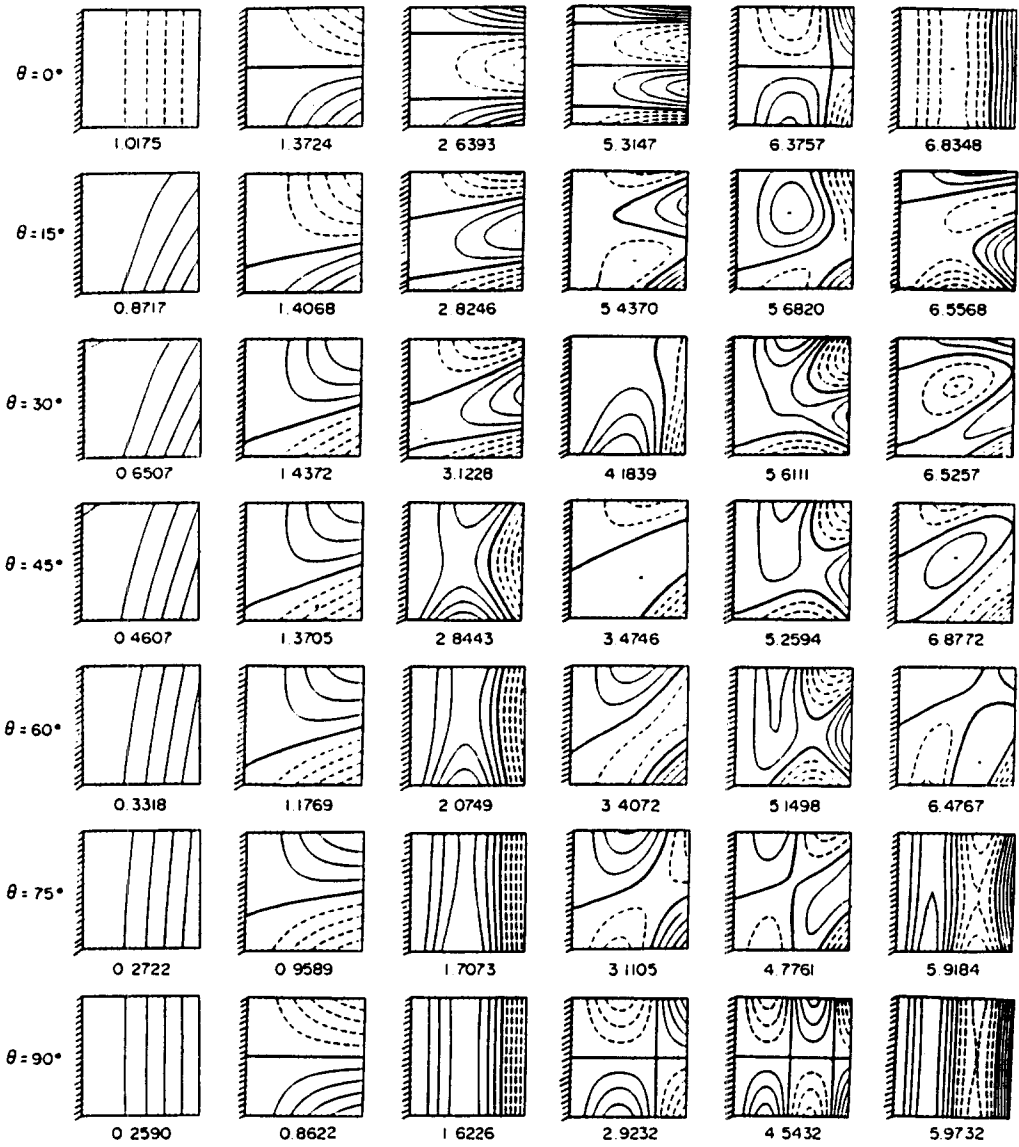


Fig. 4. Mode shapes for cantilever graphite/epoxy laminated plates.

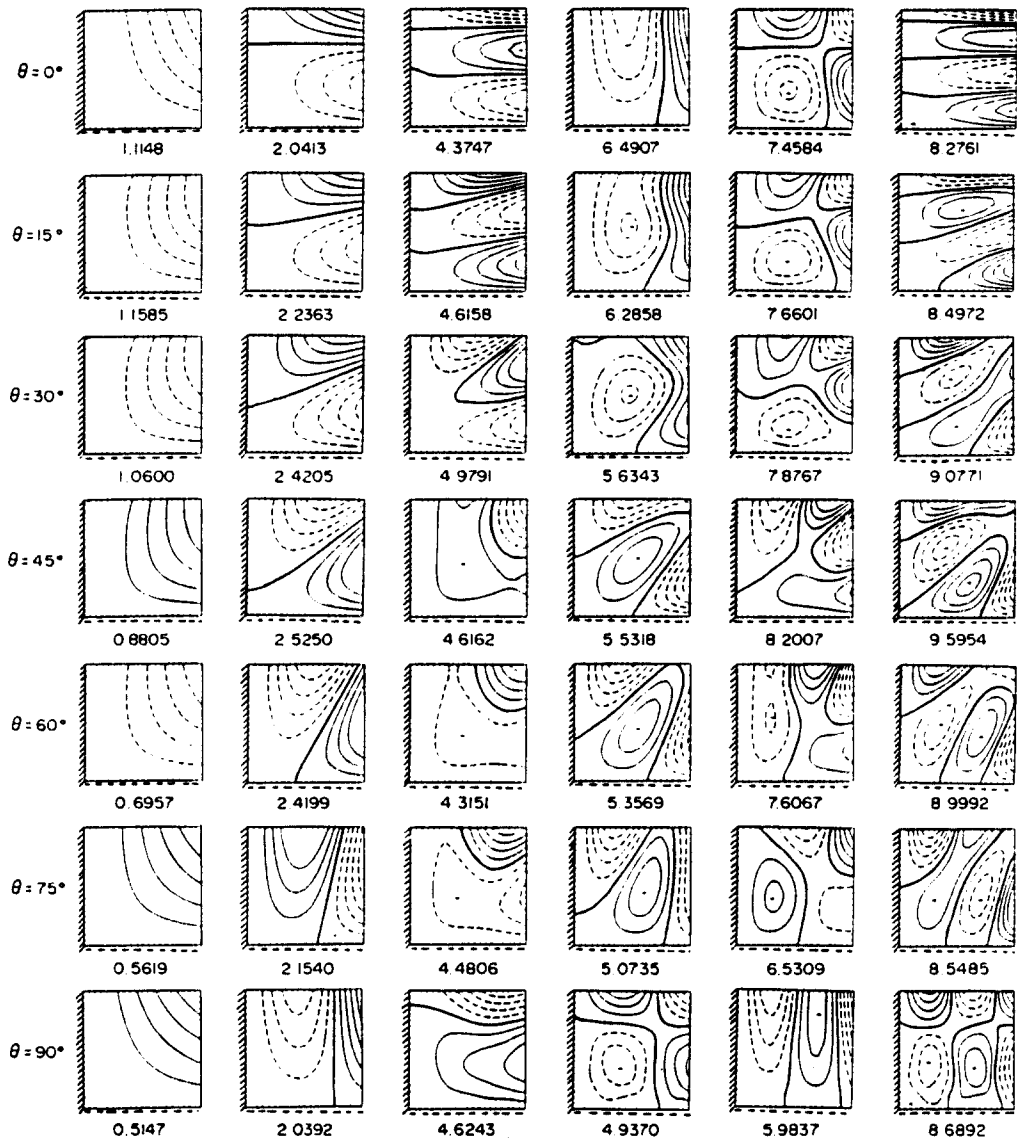


Fig. 5. Mode shapes for CSFF graphite/epoxy laminated plates.

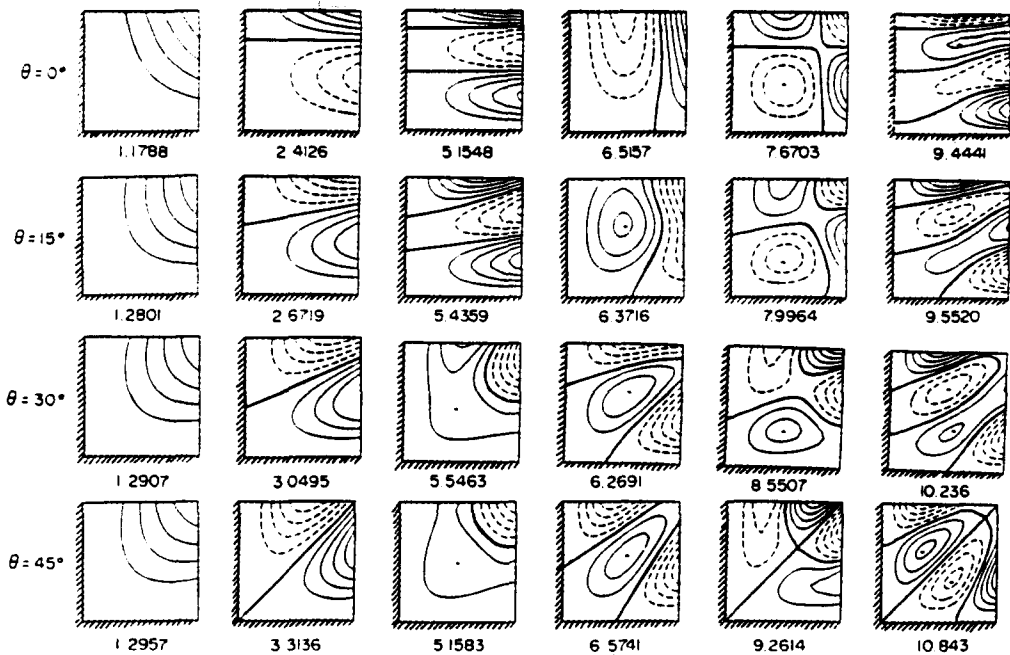


Fig. 6. Mode shapes for CCFF graphite/epoxy laminated plates.

CCFF and SSFF boundary conditions, with curve crossing being replaced by curve veering in most of the cases. For all laminates, the first mode is the double bending mode. The second mode has one nodal line in the ξ -direction for $\theta = 0$ and one nodal line in the η -direction for $\theta = 90^\circ$. For laminates with other lamination angles, the second mode has one nodal line making an angle with the ξ -axis almost the same as the lamination angle. This shows that the previously-mentioned observation of more nodal lines tend to appear in the direction of the fibers is also evident for this boundary condition.

For SSFF and CCFF plates, the mode shapes are very similar, and only those of the CCFF plate are given in Fig. 6. For these boundary conditions, symmetry about the diagonal $\xi = \eta$ exists only for isotropic and diagonally-orthotropic plates with layers making a 45° angle with the ξ -axis. For these laminates, mode shapes can be either symmetric or antisymmetric about the diagonal $\xi = \eta$. The gradual change in contour plots as the angle θ increases is evident.

6. CONCLUDING REMARKS

The Ritz method can straightforwardly be applied to investigate the vibrational characteristics of laminated plates with various edge conditions. It gives reasonably accurate results with fewer degrees of freedom than some other method like the finite element method.

It is observed that the maximum two fundamental frequencies occur at the fiber angle θ of 45° for plates with geometric symmetry about the $\xi = \eta$ diagonal line (i.e. FFFF, SSFF and CCFF plates). For plates for which the line of geometric symmetry is $\eta = 0$ (i.e. SFFF and CFFF plates) the behavior is different. For cantilever plates, it is observed that increasing the fiber orientation angle from 0° to 90° decreases the fundamental frequency, which corresponds to the first bending mode. For SFFF plates, the maximum fundamental frequency (which corresponds to the first twisting mode) occurs at the fiber angles of 45° .

Possible symmetry classes of the mode shapes has been shown. For completely-free plates, four symmetry classes have been distinguished. Symmetry classes are observed about the coordinates for cross-ply laminates and about the diagonals for 45° angle-ply laminates. Two classes of symmetry about the $\eta = 0$ axis are observed for cross-ply laminates with

SFFF and CFFF boundaries. Two classes of symmetry about the diagonal $\xi = \eta$ are observed for SSFF and CCFF plates with 45° angle-ply lamination. As expected, no symmetry has been found in the mode shapes of CSFF plates.

It has been noticed that more nodal lines tend to appear in the direction of the fibers for certain mode shapes and boundary conditions. A gradual change in the nodal lines as θ increases has been shown.

Acknowledgement—The author thanks Professor Arthur W. Leissa of the Ohio State University for reviewing the paper and giving valuable suggestions.

REFERENCES

- Jensen, D. W. and Crawley, E. F. (1984). Frequency determination techniques for cantilevered plates with bending-torsion coupling. *AIAA JI* **22**, 415-420.
- Jensen, D. W., Crawley, E. F. and Dugundji, J. (1982). Vibration of cantilevered graphite/epoxy plates with bending-torsion coupling. *J. Reinf. Plast. Compos.* **1**, 254-269.
- Jones, R. M. (1973). Buckling and vibration of unsymmetrically laminated cross-ply rectangular plates. *AIAA JI* **11**, 1626-1632.
- Leissa, A. W. (1978). Recent research in plate vibrations. 1973-1976: complicating effects. *Shock Vibr. Dig.* **10**, 21-35.
- Leissa, A. W. (1981). Recent research in plate vibrations. 1976-1980: complicating effects. *Shock Vibr. Dig.* **13**, 19-36.
- Leissa, A. W. (1987). Recent studies in plate vibrations. 1981-1985: complicating effects. *Shock Vibr. Dig.* **19**, 10-24.
- Leissa, A. W. and Narita, Y. (1989). Vibration studies for simply supported symmetrically laminated rectangular plates. *Compos. Struct.* **12**, 113-132.
- Leissa, A. W. and Qatu, M. S. (1991). Equations of elastic deformation for laminated composite shallow shells. *J. Appl. Mech.* **58**, 181-188.
- Lin, C. C. (1974). Exact solutions for free transverse vibrations of unsymmetrically laminated rectangular plates. *J. Sci. Engng* **11**, 139-152.
- Lin, C. C. and King, W. W. (1974). Free transverse vibrations of rectangular unsymmetrically laminated plates. *J. Sound Vibr.* **36**, 91-103.
- Qatu, M. S. (1989). Free vibration and static analysis of laminated composite shallow shells. Ph.D. Dissertation, The Ohio State University.
- Qatu, M. S. and Leissa, A. W. (1991a). Natural frequencies for cantilevered doubly-curved laminated composite shallow shells. *Compos. Struct.* **17**, 227-256.
- Qatu, M. S. and Leissa, A. W. (1991b). Free vibration of completely free doubly-curved laminated composite shallow shells. *J. Sound Vibr.* (to appear).
- Sivakumaran, K. S. (1987). Natural frequencies of symmetrically laminated rectangular plates with free edges. *Compos. Struct.* **7**, 191-204.
- Vinson, J. R. and Sierakowski, R. L. (1986). *The Behavior of Structures Composed of Composite Materials*. Martinus Nijhoff, Dordrecht.